

# Chemical Science

Accepted Manuscript

This article can be cited before page numbers have been issued, to do this please use: J. Jang, H. Kim and E. J. Cho, *Chem. Sci.*, 2026, DOI: 10.1039/D6SC02203K.



This is an Accepted Manuscript, which has been through the Royal Society of Chemistry peer review process and has been accepted for publication.

Accepted Manuscripts are published online shortly after acceptance, before technical editing, formatting and proof reading. Using this free service, authors can make their results available to the community, in citable form, before we publish the edited article. We will replace this Accepted Manuscript with the edited and formatted Advance Article as soon as it is available.

You can find more information about Accepted Manuscripts in the [Information for Authors](#).

Please note that technical editing may introduce minor changes to the text and/or graphics, which may alter content. The journal's standard [Terms & Conditions](#) and the [Ethical guidelines](#) still apply. In no event shall the Royal Society of Chemistry be held responsible for any errors or omissions in this Accepted Manuscript or any consequences arising from the use of any information it contains.

## ARTICLE

# Electrochemical Deoxygenative Trifluoromethylallenylation of Propargylic Alcohols via Sodium-Mediated Pre-association

Jihoon Jang,<sup>a</sup> Hyunwoo Kim<sup>b</sup> and Eun Jin Cho<sup>\*a</sup>

Received 00th January 20xx,  
Accepted 00th January 20xx

DOI: 10.1039/x0xx00000x

We report an electrochemical protocol that enables the direct conversion of free propargylic alcohols into trifluoromethylated allenes through sodium-mediated radical C–O bond activation. The transformation proceeds via a pre-association mechanism between the propargylic alcohol and a trifluoromethyl sulfinate reagent, which organizes the reactive complex through Na<sup>+</sup> coordination. This interaction lowers the energetic barrier of the intrinsically endothermic C–O bond cleavage, allowing a concerted radical addition pathway under mild electrochemical conditions. Combined experimental and computational studies, including NMR titration, kinetic analysis, and DFT calculations, reveal that sodium acts as an ion bridge, enabling selective CF<sub>3</sub> incorporation. The reaction exhibits broad substrate scope and high chemoselectivity, tolerating halogens, heteroarenes, and sensitive functional groups, and proving effective for the late-stage trifluoromethylation of natural products and pharmaceuticals.

## Introduction

Allenes, cumulated dienes with a central *sp*-hybridized carbon and two orthogonal  $\pi$ -bonds,<sup>1,2</sup> exhibit unique electronic structures that enable unusual reactivity.<sup>3</sup> These features impart a polarized  $\pi$ -system and exceptional control of regio- and stereochemistry in various transformations.<sup>4–8</sup> Consequently, allenes are not only common motifs in natural products but also versatile intermediates in the synthesis of complex pharmaceuticals and functional materials.<sup>9–11</sup> Incorporating a trifluoromethyl (CF<sub>3</sub>) group into an allene framework further enhances these attributes. The CF<sub>3</sub> group is a strongly electron-withdrawing, privileged motif in medicinal chemistry, known to improve pharmacophysical properties including metabolic stability and binding selectivity of drug candidates.<sup>12–15</sup> The synergy between the allene core and a CF<sub>3</sub> substituent creates a polarized, highly reactive  $\pi$ -system, offering a broadly useful platform for selective bond-forming reactions.

Propargylic alcohols with both an alcohol and an alkyne are valuable building blocks, enabling diverse bond constructions. A well-established two-electron approach is to convert propargylic alcohols into allenes via remote nucleophilic substitution after activating the hydroxyl into a leaving group.<sup>16–40</sup> This strategy has furnished a variety of functionalized allenes (Figure 1A).<sup>41–52</sup> However, the scope of nucleophiles in these transformations remains limited. In particular, a trifluoromethyl anion (CF<sub>3</sub><sup>–</sup>) cannot be employed in such substitutions because it is intrinsically unstable, undergoing rapid  $\alpha$ -elimination to form difluorocarbene and fluoride.<sup>53,54</sup>

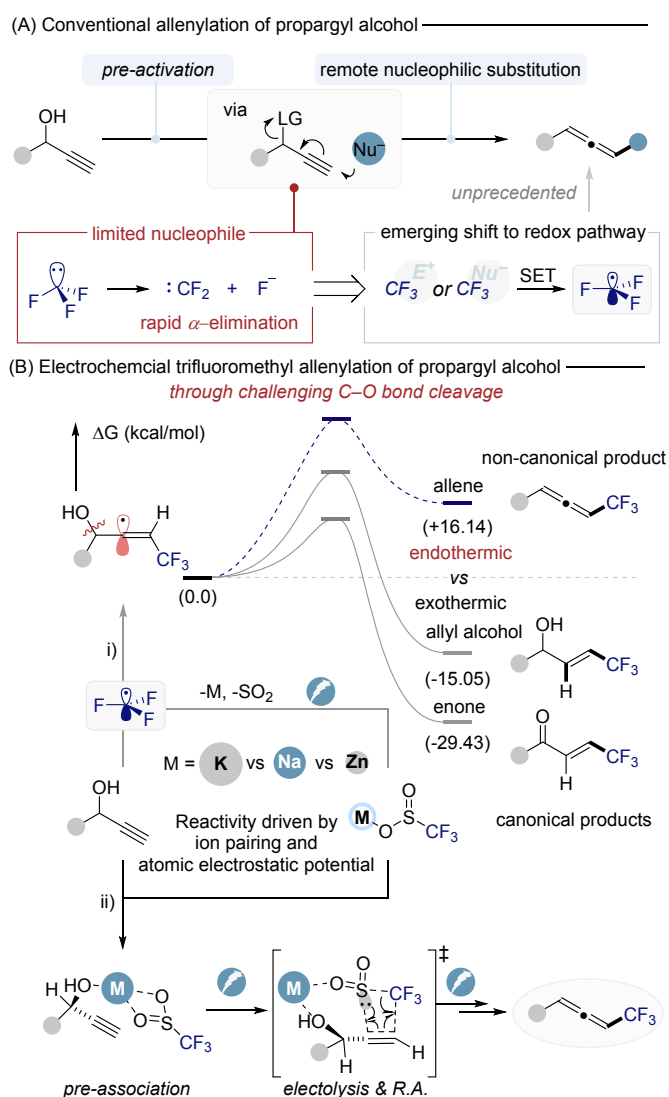


Figure 1. Allenylation of propargylic alcohol.

<sup>a</sup> Department of Chemistry, Chung-Ang University, 84 Heukseok-ro, Dongjak-gu, Seoul 06974, Republic of Korea.

<sup>b</sup> Department of Chemistry, Pohang University of Science and Technology (POSETECH), Pohang 37673, Republic of Korea.

† Electronic supplementary information (ESI) available. See DOI: 10.1039/x0xx00000x



This decomposition precludes direct nucleophilic trifluoromethylation of propargylic alcohols.

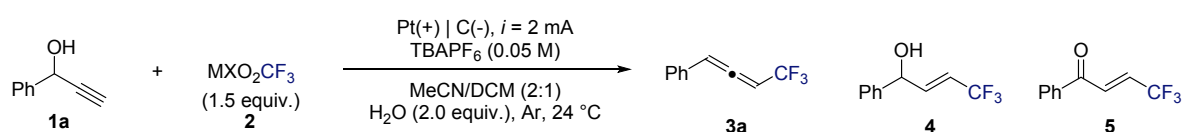
As a solution, chemists have turned to trifluoromethyl radicals as surrogates for  $\text{CF}_3^-$ , taking advantage of their greater stability and the abundance of reagents available to generate  $\text{CF}_3\cdot$ .<sup>55–57</sup> Indeed, radical trifluoromethylation has been extensively explored in many contexts, from aromatic C–H functionalization to alkene difunctionalizations, using photochemical, electrochemical, and metal-catalyzed protocols.<sup>58–69</sup> Surprisingly, however, radical trifluoromethylation of propargylic alcohols to form allenes has not been reported to date. The lack of precedent for this transformation stems from fundamental challenges in radical C–O bond activation (Figure 1B-i). Selective cleavage of a propargylic C–O bond by radical means is thermodynamically disfavored (endothermic) and must compete against more favorable pathways. For example, addition of a  $\text{CF}_3\cdot$  radical to a propargylic alkyne would generate a highly reactive vinyl radical intermediate. Vinyl radicals preferentially follow divergent pathways such as  $\beta$ -scission or hydrogen atom transfer, instead of the productive allene-forming route.<sup>70–75</sup> Consequently, the intrinsic instability of vinyl radicals, combined with the endothermic nature of C–O bond scission, constitutes a formidable mechanistic barrier to achieving trifluoromethylative allenylation under radical conditions. Herein, we report an electrochemical radical trifluoromethylation of free propargylic alcohols that overcomes these challenges, enabling the first direct synthesis of  $\text{CF}_3$ -substituted allenes (Figure 1B-ii). Central to our design is the *in situ* pre-activation of the alcohol through coordination

with a  $\text{CF}_3$  radical source. We envisioned that a reagent such as  $\text{MSO}_2\text{CF}_3$  (metal trifluoromethylsulfonate) could engage in hydrogen bonding or Lewis acid–base coordination with the –OH group, thereby weakening the C–O bond prior to cleavage. Upon electrochemical anodic oxidation, the  $\text{CF}_3$  source generates  $\text{CF}_3$  radicals that attack the alkyne and, crucially, induce C–O bond dissociation to form the allene.

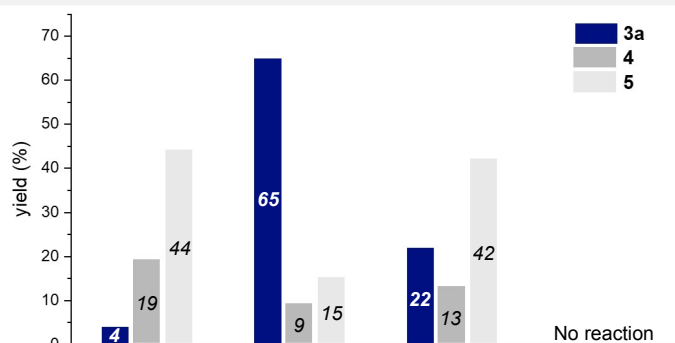
Notably, the coordinated  $\text{CF}_3$ –alcohol complex lowers the energy barrier enough to drive what is an endothermic bond cleavage into a productive pathway. The reaction proceeds with high regio- and chemoselectivity, affording trifluoromethylated allenes in good yield. Combined experimental and DFT studies support the formation of the alcohol– $\text{CF}_3$  complex and its role in guiding the reaction toward allene formation, a transformation that was previously considered infeasible.

## Results and discussion

To prove the critical role of substrate–reagent pre-association in the formation of  $\text{CF}_3$ -substituted allenes, we began our investigation by screening various  $\text{MXO}_2\text{CF}_3$  reagents using 1-phenylprop-2-yn-1-ol (**1a**) as a model substrate (Scheme 1A). Electrolysis was conducted under constant current (2 mA) conditions with  $n\text{Bu}_4\text{NPF}_6$  as the electrolyte, a platinum anode, and a graphite cathode in MeCN/DCM (2:1) containing  $\text{H}_2\text{O}$  (2.0 equiv.) as an additive. Gratifyingly, trifluoromethylated allenes (**3a**) were formed in good yield. The nature of the counter cation proved crucial.



A)  $\text{CF}_3$  reagent variations



|                           | <b>2a</b> | <b>2b</b> | <b>2c</b> | <b>2d</b> |
|---------------------------|-----------|-----------|-----------|-----------|
| ion size (Å)              | 1.38      | 1.02      | 0.74      | 1.02      |
| $E_p$ ox. (V vs. Ag/AgCl) | 1.00      | 0.96      | 1.14      | 2.40      |

B) Further optimization parameters

| Entry          | Variations with <b>2b</b>                   | Yield (%) ( <b>3a/4/5</b> ) |
|----------------|---|-----------------------------|
| 1              | None ( $Q = 2.24$ F/mol, $FE = 89\%$ )      | 65/9/15                     |
| 2              | No electricity                              | N.R.                        |
| 3              | MeCN instead of MeCN/DCM (2:1)              | 21/2/15                     |
| 4              | DMF instead of MeCN/DCM (2:1)               | 0/2/19                      |
| 5              | DMSO instead of MeCN/DCM (2:1)              | 0/4/27                      |
| 6              | MeCN/DCM, (1.5:1) instead of MeCN/DCM (2:1) | 24/5/17                     |
| 7              | MeCN/DCM, (3:1) instead of MeCN/DCM (2:1)   | 26/6/26                     |
| 8 <sup>c</sup> | BDD(+) instead of Pt(+)                     | 62/8/19                     |
| 9              | RVC(+) instead of Pt(+)                     | 0/25/24                     |
| 10             | $i = 1$ mA                                  | 37/0/2                      |
| 11             | $i = 2.5$ mA                                | 59/15/18                    |
| 12             | $U_{\text{cell}} = 3.0$ V                   | 0/0/0                       |
| 13             | $U_{\text{cell}} = 3.5$ V                   | 61/5/14                     |
| 14             | $U_{\text{cell}} = 4.0$ V                   | 30/8/35                     |
| 15             | no $\text{H}_2\text{O}$ added               | 45/3/12                     |
| 16             | $\text{H}_2\text{O}$ 1 equiv.               | 49/3/9                      |
| 17             | $\text{H}_2\text{O}$ 3 equiv.               | 60/8/19                     |

**Scheme 1.** Optimization of reaction parameters.<sup>a,b</sup> Reactions were conducted on 0.2 mmol scale. <sup>c</sup>Yields were determined by <sup>19</sup>F NMR spectroscopy using 2,2,2-trifluoroethanol as an internal standard.



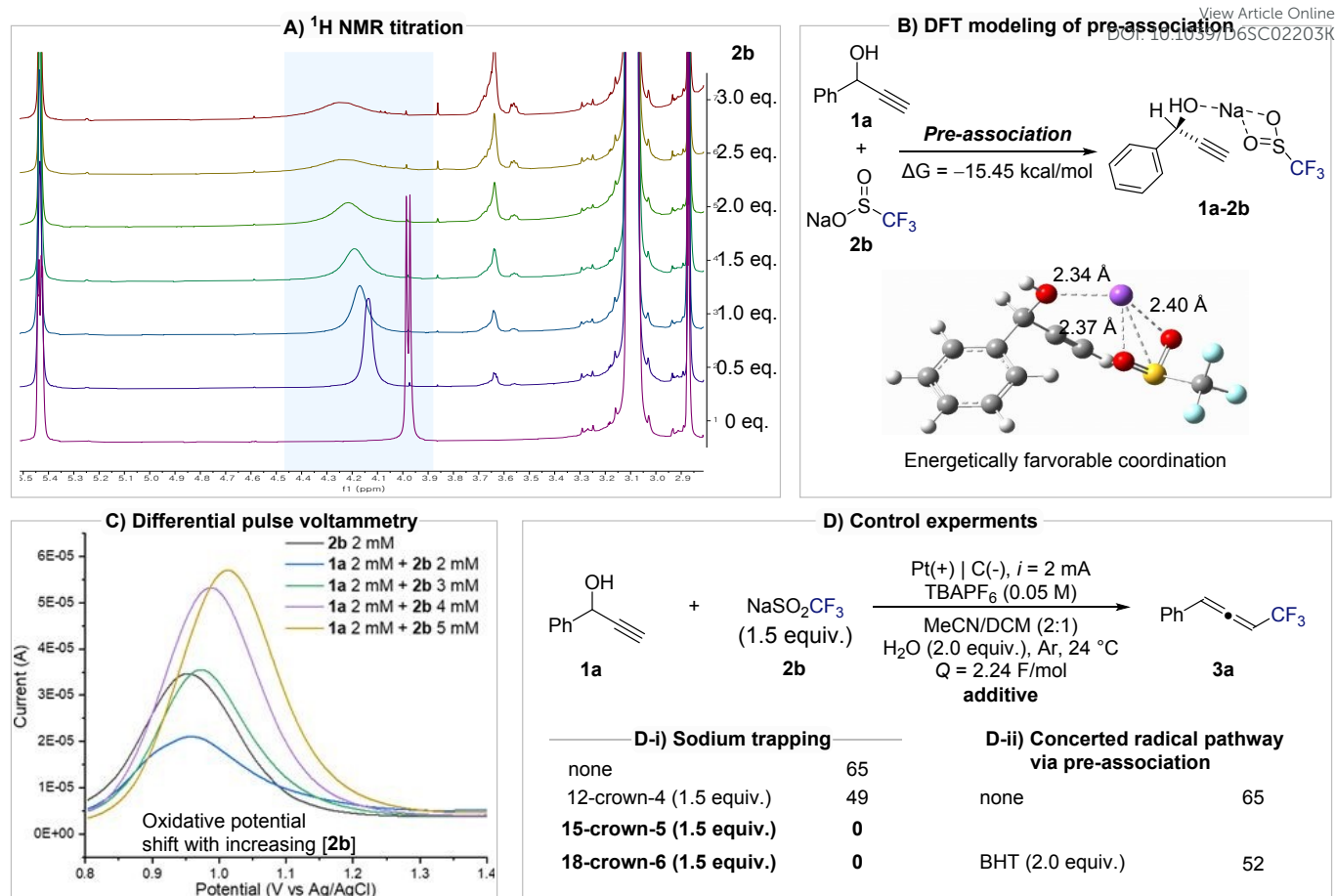


**Figure 2.** Evidence and implication of sodium cation assisted pre-association in electrochemical allenylation. a)  $^1\text{H}$  NMR titration experiment: **1a** (1.0 equiv.), **2b** (x equiv.) TBAPF<sub>6</sub> (1.0 equiv.) H<sub>2</sub>O (2.0 equiv.) in CD<sub>3</sub>CN solvent. b) DFT calculations were performed at the M062X/def2TZVP/PCM in MeCN level of theory. Free energy given in kcal/mol. c) Differential pulse voltammetry of **2b**, and mixture of **1a** with **2b**. d) Results of control experiments.

Among Na<sup>+</sup>, K<sup>+</sup>, and Zn<sup>2+</sup> salts, NaSO<sub>2</sub>CF<sub>3</sub> (**2b**) delivered **3a** in 65% yield, whereas KSO<sub>2</sub>CF<sub>3</sub> (**2a**) and Zn(SO<sub>2</sub>CF<sub>3</sub>)<sub>2</sub> (**2c**) primarily generated the competing allylic alcohol (**4**) or enone (**5**) byproducts. These results indicate that cation size significantly influences the geometry and strength of the pre-association between the CF<sub>3</sub> reagent and the alcohol. Notably, the oxidation potentials of **2a–2c** differ only slightly, suggesting that the distinct product selectivities arise not from redox differences but from differences in their coordination environments. Taken together, these findings strongly support the formation of a substrate–reagent pre-association complex that governs the selective allene formation. In contrast, the carboxylate analogue NaCO<sub>2</sub>CF<sub>3</sub> (**2d**) was completely unreactive under identical conditions, with no detectable conversion of **1a**. This inactivity is attributed to its considerably higher oxidation potential, which precludes electrochemical generation of CF<sub>3</sub> radicals. The divergent reactivity between sulfonates and carboxylates highlights the delicate interplay between reagent redox properties and pre-association effects in enabling endothermic C–O bond activation under electrochemical radical conditions. With NaSO<sub>2</sub>CF<sub>3</sub> (**2b**) identified as the optimal CF<sub>3</sub> source, we next examined the influence of reaction parameters (Scheme 1B). Control experiments confirmed that no product

formation occurred in the absence of electrical input, highlighting the essential role of electrolysis in the transformation (entry 2). Solvent effects were pronounced that the use of MeCN, DMF, or DMSO as single solvents or deviation from the 2:1 MeCN/DCM ratio led to markedly reduced yields or complete loss of reactivity (entries 3–7). The nature of the anode also proved critical. Replacement of the platinum anode with boron-doped diamond (BDD) maintained comparable efficiency, affording **3a** in 61% yield (entry 8). In contrast, the use of a graphite anode completely suppressed allene formation, producing the allylic alcohol (**4**) and enone (**5**) byproducts (entry 9). Current intensity exerted a notable influence. Lowering the current to 1 mA resulted in incomplete conversion of **1a** (≈ 60%), while higher currents caused slight decreases in yield, likely due to overoxidation of intermediates (entries 10–11). Constant-potential electrolysis further clarified the relationship between oxidation potential and efficiency. At 3.0 V, no conversion of **1a** was observed, consistent with an insufficient anodic potential to initiate oxidation (entry 12). Increasing the potential to 3.5 V restored productive reactivity comparable to that under constant-current conditions (entry 13), whereas potentials above 3.5 V led to significant yield erosion, attributed to oxidative degradation of **3a** into



overoxidized byproducts such as **5** (entry 14).<sup>76</sup> Finally, varying the water loading between 1.0 and 3.0 equiv. resulted in only

marginal changes in yield (entries 15–17), indicating a subtle yet reproducible influence of water on the overall efficiency.

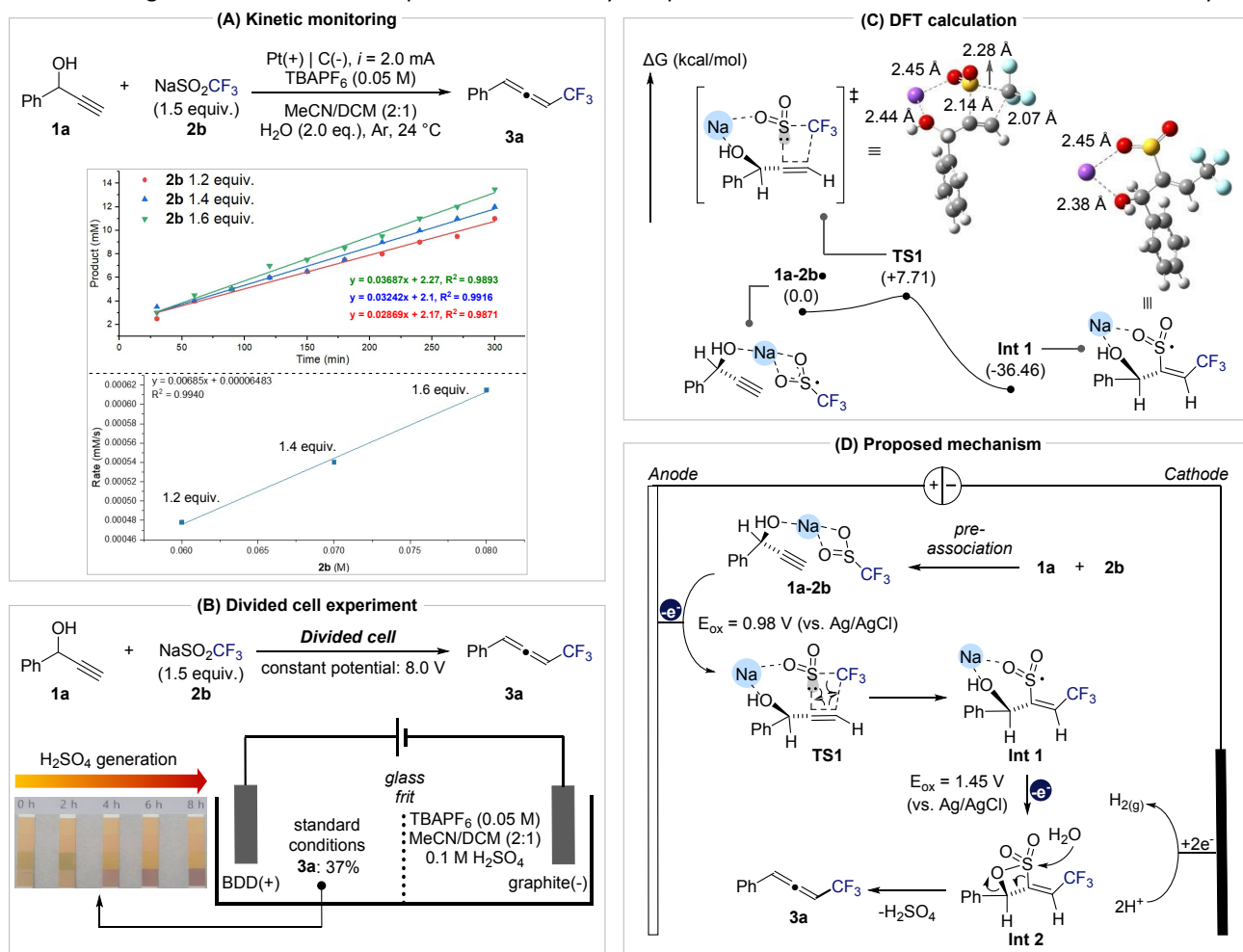


**Figure 3.** Mechanistic investigations. A) Variations of **2b**'s equivalent with standard condition. Reaction monitoring was proceeded by <sup>19</sup>F NMR using 2,2,2-trifluoroethanol as an internal standard. B) Cyclic voltammetry of reaction components. C) Result of the divided cell experiment. D) Computed relative free energies of transition state for concerted radical addition step. DFT calculations were performed at the M062X/def2TZVP/PCM in MeCN level of theory. Free energy given in kcal/mol. E) Proposed mechanism based on mechanistic investigations.

To elucidate the mechanism and validate the formation of a pre-association complex between **1a** and **2b**, a series of spectroscopic, electrochemical, and kinetic experiments were conducted (Figure 2). NMR titration experiments revealed clear evidence of substrate–reagent interaction. Upon incremental addition of **2b** to **1a**, the O–H peak of **1a** shifted progressively downfield and broadened, consistent with coordination between the hydroxyl oxygen and the sodium cation of **2b** (Figure 2A). DFT calculations indicated that the pre-association of **1a** and **2b** via Na<sup>+</sup> coordination is energetically favorable ( $\Delta G = -15.45 \text{ kcal mol}^{-1}$ ; Figure 2B). Differential pulse voltammetry (DPV) further supported complex formation. The oxidation potential of **2b** increased systematically with [**2b**], suggesting that the redox behavior of **2b** is modulated by its association with **1a** (Figure 2C). Cyclic voltammetry provided further evidence. While individual scans of **1a** or **2b** showed no significant oxidation waves, their mixture exhibited new redox features. In particular, the oxidation signal of **1a** diminished and disappeared, indicating that pre-association between **1a** and **2b**

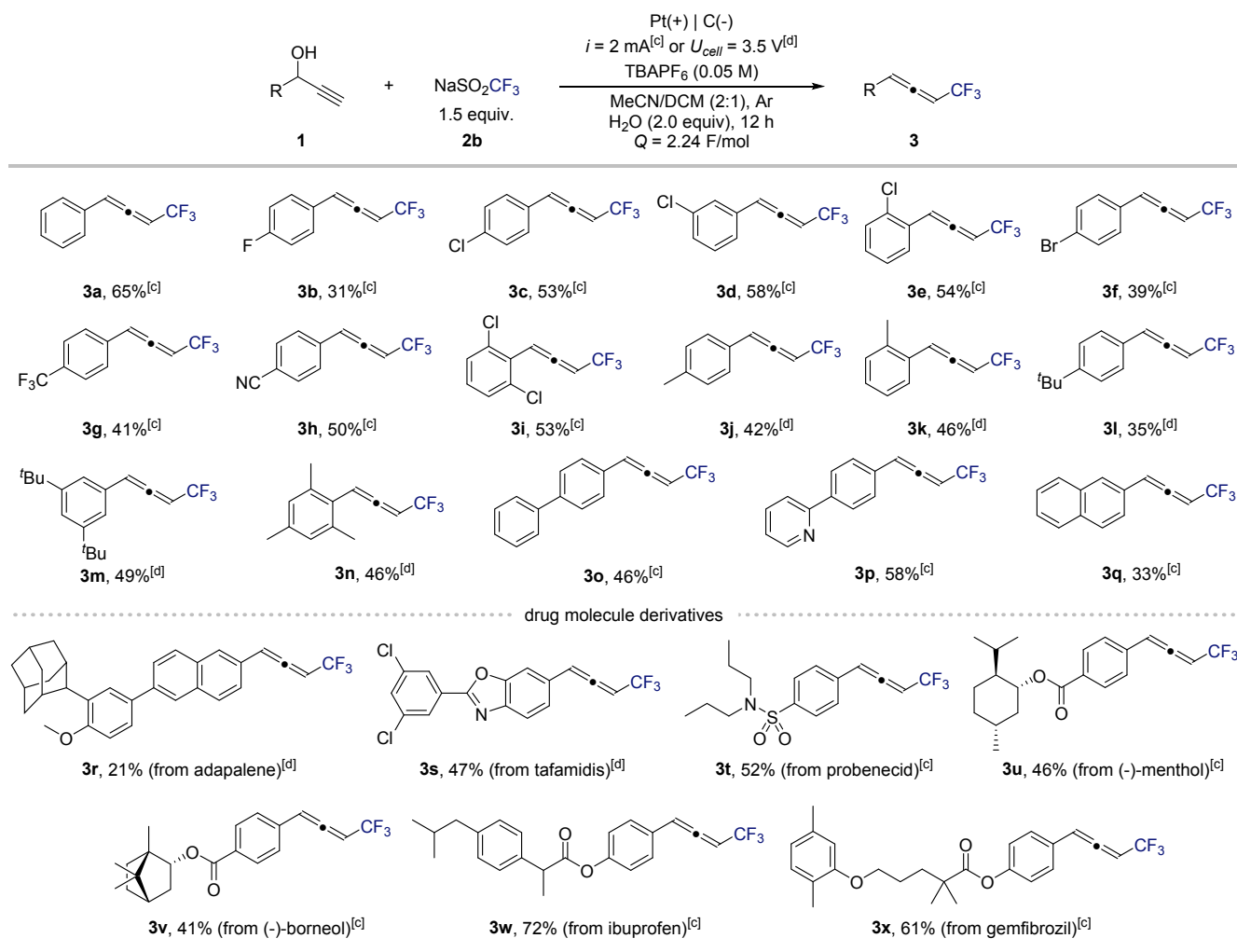
is mechanistically relevant (see Figure S2 in the supporting information). The importance of sodium in mediating this pre-association was confirmed by crown ether experiments (Figure 2D-i). In the presence of the weak sodium chelator 12-crown-4, the yield of **3a** decreased slightly (49%), whereas stronger complexants such as 15-crown-5 and 18-crown-6 completely inhibited product formation. These results clearly demonstrate that sodium acts as an ion-bridge, organizing the propargyl alcohol and CF<sub>3</sub> source into a reactive complex. To investigate the reaction pathway during the radical addition step, we conducted control experiments using radical inhibitors BHT (butylated hydroxytoluene) and TEMPO (2,2,6,6-tetramethylpiperidine 1-oxyl). Notably, the addition of BHT did not significantly suppress product formation (52% yield), suggesting that free CF<sub>3</sub> radicals are not involved as discrete intermediates and that the transformation proceeds via a concerted radical addition pathway (Figure 2D-ii). In contrast, in the presence of TEMPO, the reaction predominantly resulted in oxidation of **1a** to the corresponding ketone (see Scheme S1 in



the supporting information). This outcome is attributed to the well-established ability of TEMPO to undergo electrochemical

oxidation to generate oxyl radical species, which can mediate alcohol oxidation.<sup>77</sup>

DOI: 10.1039/D6SC02203K



**Scheme 2.** Substrate scope of electrochemical trifluoromethyl allenylation of propargyl alcohols.<sup>a,b</sup> Reactions were conducted on 0.3 mmol scale. <sup>c</sup>Yields were determined by <sup>19</sup>F NMR using 2,2,2-trifluoroethanol as an internal standard. <sup>d</sup>Reactions were carried out under constant current condition. <sup>e</sup>Reactions were carried out under constant potential condition.

Notably, the addition of the radical scavenger BHT did not suppress product formation (52% yield), indicating that free CF<sub>3</sub> radicals are not really involved and that the transformation proceeds via a concerted radical addition pathway. Kinetic analysis further clarified the mechanistic relevance of this pre-association (Figure 3A). Monitoring product accumulation under varying concentrations of **2b** while keeping [**1a**] constant revealed a linear relationship between initial rate and [**2b**] (R<sup>2</sup> = 0.994), consistent with a first-order dependence on **2b**. This result indicates that **2b** participates directly in the rate-determining step. A divided-cell experiment confirmed that this transformation originates from anodic processes, as product formation was observed exclusively in the anodic compartment, thereby ruling out cathodic reduction pathways such as vinyl radical formation followed by E1cB-type elimination (Figure 3B and the Supporting Information for further details). In addition, monitoring the pH of the anodic solution revealed a gradual

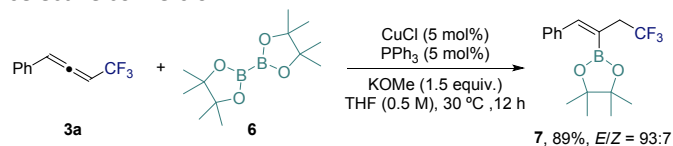
acidification over the course of the reaction, consistent with the generation of H<sub>2</sub>SO<sub>4</sub>. The generated acid does not appear to affect the reactivity of the system. When the isolated product **3a** was subjected to H<sub>2</sub>SO<sub>4</sub> conditions, no decomposition or transformation was observed (Figure S5 in the supporting information). Furthermore, under the undivided cell conditions employed in this study, the protons generated at the anode are expected to be reduced at the cathode, thereby completing the redox cycle and preventing the accumulation of acidic species. To gain deeper insight into the C–O activation step, DFT calculations were performed on the oxidation and radical addition sequence (Figure 3C). After anodic oxidation of the pre-associated **1a–2b** complex, radical addition of CF<sub>3</sub> to the terminal carbon of the alkyne is facilitated by an ion-bridging interaction between the hydroxyl group and Na<sup>+</sup>, positioning the sulfonyl group for concerted CF<sub>3</sub>/SO<sub>2</sub> coupling to form



intermediate **Int-1**. Based on these results, a mechanistic model is proposed (Figure 3D).

The propargylic alcohol (**1a**) and NaSO<sub>2</sub>CF<sub>3</sub> (**2b**) first form a pre-associated complex that undergoes anodic oxidation at 0.98 V vs Ag/AgCl to generate radical species (**1a-2b•**). This intermediate proceeds through transition state **TS1** ( $\Delta G^\ddagger = +7.71$  kcal mol<sup>-1</sup>) to yield **Int-1** ( $\Delta G = -36.46$  kcal mol<sup>-1</sup>) via a concerted radical addition. A subsequent anodic oxidation at 1.45 V produces **Int-2**, which, upon nucleophilic attack of water at the sulfonyl group, releases H<sub>2</sub>SO<sub>4</sub> and furnishes the trifluoromethylated allene **3a**. The H<sub>2</sub>SO<sub>4</sub> generated in this step provides protons that undergo reduction at the cathode, thereby maintaining charge balance in the electrochemical cell and completing the overall redox cycle.

Next, to evaluate the generality of this electrochemical protocol, we examined a diverse range of propargylic alcohols (Scheme 2). Under standard conditions, substrates bearing electron-withdrawing or neutral substituents underwent smooth conversion to the corresponding CF<sub>3</sub>-substituted allenes. In contrast, electron-rich substrates were prone to overoxidation of the allene products under constant-current conditions. Switching to constant-potential electrolysis effectively suppressed this undesired oxidation, ensuring high selectivity (also see Scheme 1b, entry 13). The methodology exhibited broad functional-group tolerance. Halogenated substrates, including fluoro (**3b**), chloro (**3c-3e**, **3i**), and bromo (**3f**) derivatives, afforded the desired products in excellent yields. Strongly electron-withdrawing substituents such as trifluoromethyl (**3g**) and cyano (**3h**) groups were also well tolerated. For electron-donating substituents (**3j-3n**), the corresponding allenes were obtained in high yields under the modified constant-potential conditions. Substrates containing extended  $\pi$ -systems or heteroaromatic motifs, including biphenyl (**3o**), pyridyl (**3p**), and naphthyl (**3q**), participated readily, highlighting the compatibility of this method with conjugated frameworks. To further demonstrate synthetic utility, late-stage trifluoromethylation of complex molecules was explored. Natural-product-derived and drug-like scaffolds such as adapalene (**3r**), tafamidis (**3s**), and a probenecid analogue (**3t**) underwent smooth transformation to their corresponding CF<sub>3</sub>-allenes. Similarly, benzoate- and acetoxy-functionalized natural products including menthol (**3u**) and (+)-borneol (**3v**) reacted efficiently. Widely used pharmaceuticals such as ibuprofen (**3w**) and gemfibrozil (**3x**) also underwent selective conversion.



Scheme 3. Application of CF<sub>3</sub>-allene **3a**: Cu-catalyzed hydroboration.<sup>78</sup>

As highlighted in the Introduction, CF<sub>3</sub>-allenes can serve as versatile building blocks for further transformations. To demonstrate this potential, we investigated the hydroboration of **3a** using bis(pinacolato)diborane (**6**) under copper catalysis

(Scheme 3). Notably, this transformation provides an alkenyl boronate bearing an allylic CF<sub>3</sub> moiety (**7**), which differs from products reported under related copper-catalyzed hydroboration conditions.<sup>78</sup> This result highlights the potentially unique reactivity of CF<sub>3</sub>-substituted allenes.

## Conclusions

In summary, we have developed an electrochemical strategy for the selective conversion of free propargylic alcohols into CF<sub>3</sub>-substituted allenes through sodium-mediated radical C–O bond activation. This transformation achieves a formally endothermic C–O bond cleavage under mild electrochemical conditions by exploiting a pre-association mechanism between the substrate and the CF<sub>3</sub> source. Systematic mechanistic investigations, combining NMR, electrochemical, kinetic, and DFT analyses, revealed that the Na<sup>+</sup> ion serves as an ion-bridge, preorganizing the propargyl alcohol and CF<sub>3</sub> reagent into a reactive complex that undergoes concerted radical addition upon anodic oxidation. This method exhibits broad substrate scope, high chemoselectivity, and excellent functional-group tolerance, enabling late-stage trifluoromethylation of complex molecules. Beyond providing a synthetically practical route to CF<sub>3</sub>-substituted allenes, this work establishes a general strategy for activating strong C–O bonds via reagent–substrate preorganization, expanding the conceptual landscape of electrochemical radical chemistry.

## Author contributions

J. J. performed synthetic and mechanistic studies. H. K. and E. J. C. coordinated the experiments and analyses. J. J. and E. J. C. analyzed the experimental data and wrote the manuscript.

## Conflicts of interest

There are no conflicts to declare.

## Data availability

The data underlying this study are available in the published article and its ESI.

## Acknowledgements

We gratefully acknowledge the National Research Foundation of Korea (RS-2024-00409659 and RS-2025-00559692) and the Ministry of Trade, Industry and Energy, Korea (Technology Innovation Program, RS-2023-00266039).

## Notes and references

- C. H. Hendon, A. T. Murray, D. R. Carbery, A. R. Walsh, *Chem. Sci.* 2013, **4**, 4278-4284.
- M. H. Palmer, *Chem. Phys.* 2006, **326**, 631-640.
- E. Soriano, I. Fernández, *Chem. Soc. Rev.* 2014, **43**, 3041-3105.



- 4 X.-L. Han, P.-P. Lin, Q. Li, *Chin. Chem. Lett.* 2019, **30**, 1495–1502.
- 5 B. Yang, Y. Qiu, J.-E. Bäckvall, *Acc. Chem. Res.* 2018, **51**, 1520–1531.
- 6 G. Qiu, J. Zhang, K. Zhou, J. Wu, *Tetrahedron* 2018, **74**, 7290–7301.
- 7 C. S. Adams, C. D. Weatherly, E. G. Burke, J. M. Schomaker, *Chem. Soc. Rev.* 2014, **43**, 3136–3163.
- 8 S. Ma, *Chem. Rev.* 2005, **105**, 2829–2872.
- 9 J. Singh, A. Sharma, A. Sharma, *Org. Front. Chem.* 2021, **8**, 5651–5667.
- 10 P. Rivera-Fuentes, F. Diederich, *Angew. Chem., Int. Ed.* 2012, **51**, 2818–2828.
- 11 A. Hoffmann-Röder, N. Krause, *Angew. Chem., Int. Ed.* 2004, **43**, 1196–1216.
- 12 N. A. Meanwell, *J. Med. Chem.* 2018, **61**, 5822–5880.
- 13 J. Wang, M. Sánchez-Roselló, J. L. Aceña, C. Pozo, A. E. Sorochinsky, S. Fustero, V. A. Soloshonok, H. Liu, *Chem. Rev.* 2014, **114**, 2432–2506.
- 14 S. Purser, P. R. Moore, S. Swallow, V. Gouverner, *Chem. Soc. Rev.* 2008, **37**, 320–330.
- 15 L. Müller, C. Faeh, F. Diederich, *Science*, 2007, **317**, 1881–1886.
- 16 J. Chao, R. Yang, J. Huang, X. Chen, X.-R. Song, Q. Xiao, *Org. Biomol. Chem.* 2025, **23**, 8862–8890.
- 17 K. Negesh, N. S. Reddy, S. Kareem, S. R. Vali, B. V. S. Reddy, *Org. Biomol. Chem.* 2025, **23**, 6665–6682.
- 18 S. Kim, D. S. Lee, N. Iqbal, J. Bae, H. S. Hwang, D. Baek, S. Hong, E. J. Cho, *Chem. Catal.* 2024, **4**, 101082.
- 19 S. Mishra, S. Raikwar, B. Baire, *Chem. Asian J.* 2023, **18**, e202300316.
- 20 F. Doraghi, A. M. Mahdavian, S. Karimian, B. Larijani, M. Mahdavi, *Adv. Synth. Catal.* 2023, **365**, 2991–3019.
- 21 S. Jiang, H. Ma, R. Yang, X.-R. Song, Q. Xiao, *Org. Chem. Front.* 2022, **9**, 5643–5674.
- 22 Z. Xiaozheng, L. Qinqin, C. Guiyan, Z. Xiaolong, S. Yingpeng, *Chin. J. Org. Chem.* 2022, **42**, 2605–2629.
- 23 J. Wu, Q. Guo, H. Hong, R. Xie, N. Zhu, *J. CO<sub>2</sub> Util.* 2022, **65**, 102192.
- 24 X.-Y. Liu, Y.-L. Liu, L. Chen, *Adv. Synth. Catal.* 2020, **362**, 5170–5194.
- 25 Z. Wang, X. Lin, X. Chen, P. Li, W. Li, *Org. Chem. Front.* 2021, **8**, 3469–3474.
- 26 W.-R. Zhu, Q. Su, H.-J. Diao, E.-X. Wang, F. Wu, Y.-L. Zhao, J. Weng, G. Lu, *Org. Lett.* 2020, **22**, 6873–6878.
- 27 G. R. Kumar, M. Rajesh, S. Lin, S. Liu, *Adv. Synth. Catal.* 2020, **362**, 5238–5256.
- 28 H. Qian, D. Huang, Y. Bi, G. Yan, *Adv. Synth. Catal.* 2019, **361**, 3240–3280.
- 29 T. Khan, S. Yaragorla, *Eur. J. Org. Chem.* 2019, 3989–4012.
- 30 F. Noël, V. D. Vuković, J. Yi, E. Richmond, P. Kravljanić, J. Moran, *J. Org. Chem.* 2019, **84**, 15926–15947.
- 31 A. Boreux, G. H. Lonca, O. Riant, F. Gagosz, *Org. Lett.* 2016, **18**, 5162–5165.
- 32 B. R. Ambler, S. Peddi, R. A. Altman, *Org. Lett.* 2015, **17**, 2506–2509.
- 33 Y.-L. Ji, J.-J. Kong, J.-H. Lin, J.-C. Xiao, Y.-C. Gu, *Org. Biomol. Chem.* 2014, **12**, 2903–2906.
- 34 T. S. N. Zhao, K. J. Szabó, *Org. Lett.* 2012, **14**, 3966–2969.
- 35 T. Yamazaki, Y. Watanabe, N. Yoshida, T. Kawasaki-Takasaka, *Tetrahedron* 2012, **68**, 6665–6673.
- 36 P. Li, Z.-J. Liu, J.-T. Liu, *Tetrahedron* 2010, **66**, 9729–9732.
- 37 Y. Watanabe, T. Yamazaki, *Synlett* 2009, **20**, 3352–3354.
- 38 M. Shimizu, M. Higashi, Y. Takeda, G. Jiang, M. Murai, T. Hiyama, *Synlett* 2007, **7**, 1163–1165.
- 39 T. Yamazaki, T. Yamamoto, R. Ichihara, *J. Org. Chem.* 2006, **71**, 6251–6253.
- 40 T. Sakamoto, K. Takahashi, T. Yamazaki, T. Kitazume, *J. Org. Chem.* 1999, **64**, 9467–9474.
- 41 C. Beluze, T. Hu, D. Bouyssi, N. Monteiro, A. Amgoune, *Synthesis* 2025, **57**, 2935–2945. DOI: 10.1039/D6SC02203K
- 42 B.-Y. Xiao, W. Huang, F.-H. Zhang, *Eur. J. Org. Chem.* 2025, **28**, e202500302.
- 43 L. Gan, X. Wan, Y. Pang, Y. Zou, Y.-H. Deng, Z. Shao, *Org. Chem. Front.* 2025, **12**, 1001–1064.
- 44 R. Lin, Y. Zhang, T. Xiong, H. Huang, X. Peng, Y. Zhang, N. Huang, W. Hu, J. Jiang, *ACS Catal.* 2025, **15**, 16236–16246.
- 45 S. Yaragorla, A. Shaik, D. S. Latha, *J. Org. Chem.* 2025, **90**, 4735–4747.
- 46 Z. Chen, H. Qian, *Org. Lett.* 2025, **27**, 522–527.
- 47 H. Chang, R. Wang, Y.-M. Wang, *Chem. Asian J.* 2025, **20**, e00105.
- 48 Y. Xia, M. Liu, W. Li, P. Li, *Asian J. Org. Chem.* 2024, **13**, e202400377.
- 49 C. Jarava-Barrera, A. Parra, S. Quesada, S. Orgaz-Gordillo, R. F. Pradilla, A. Viso, J. Teresa, I. Alonso, M. Tortosa, *Adv. Synth. Catal.* 2024, **366**, 768–773.
- 50 W. Xiao, J. Wu, *Org. Chem. Front.* 2022, **9**, 5053–5073.
- 51 S. Du, A.-X. Zhou, R. Yang, X.-R. Song, Q. Xiao, *Org. Chem. Front.* 2021, **8**, 6760–6782.
- 52 S. Wu, X. Huang, C. Fu, S. Ma, *Org. Chem. Front.* 2017, **4**, 2002–2007.
- 53 Y. Fujihira, Y. Liang, M. Ono, K. Hirano, T. Kagawa, N. Shibata, *Beilstein J. Org. Chem.* 2021, **17**, 431–438.
- 54 T. Saito, J. Wang, E. Tokunaga, S. Tsuzuki, N. Shibata, *Sci. Rep.* 2018, **8**, 11501.
- 55 R. Giri, A. J. Fernandes, D. Katayev, *Acc. Chem. Res.* 2025, **58**, 2046–2060.
- 56 M. Duan, Q. Shao, Q. Zhou, P. S. Baran, K. N. Houk, *Nat. Commun.* 2024, **15**, 4630.
- 57 H. Xiao, Z. Zhang, Y. Fang, L. Zhu, C. Li, *Chem. Soc. Rev.* 2021, **50**, 6308–6319.
- 58 S. Kim, H. Kim, *ACS Catal.* 2025, **15**, 6826–6851.
- 59 R. Shaw, N. Sihag, H. Bhartiya, M. R. Yadav, *Org. Chem. Front.* 2024, **11**, 954–1014.
- 60 S. Kim, H. Kim, *J. Am. Chem. Soc.* 2024, **146**, 22498–22508.
- 61 Y. Ouyang, F.-L. Qing, *J. Org. Chem.* 2024, **89**, 2815–2824.
- 62 C. H. Ka, S. Kim, E. J. Cho, *Chem. Rec.* 2023, **23**, e202300036.
- 63 Z. Zou, W. Zhang, Y. Wang, Y. Pan, *Org. Chem. Front.* 2021, **8**, 2786–2798.
- 64 R. P. Bhaskaran, B. P. Babu, *Adv. Synth. Catal.* 2020, **362**, 5219–5237.
- 65 F. Ye, F. Berger, H. Jia, J. Ford, A. Wortman, J. Börgel, C. Genicot, T. Ritter, *Angew. Chem. Int. Ed.* 2019, **58**, 14615–14619.
- 66 E. H. Oh, H. J. Kim, S. B. Han, *Synthesis* 2018, **50**, 3346–3358.
- 67 T. Chatterjee, N. Iqbal, Y. You, E. J. Cho, *Acc. Chem. Res.* 2016, **49**, 2284–2294.
- 68 E. J. Cho, *Chem. Rec.* 2016, **16**, 47–63.
- 69 C. Ni, M. Hu, J. Hu, *Chem. Rev.* 2015, **116**, 765–825.
- 70 N. Tang, S. Chen, C. Li, P. Du, W. Yang, R. Qiu, *ACS Catal.* 2025, **15**, 11062–11073.
- 71 M. Liang, H. Ma, X.-R. Song, Q. Xiao, *Adv. Synth. Catal.* 2024, **366**, 2659–2677.
- 72 P. Bovonsombat, P. Sophanpanichkul, S. Losuwanakul, *RSC Adv.* 2022, **12**, 22678–22694.
- 73 B. Zhang, T. Wang, *Asian J. Org. Chem.* 2018, **7**, 1758–1783.
- 74 R. K. Kumar, X. Bi, *Chem. Commun.* 2016, **52**, 853–868.
- 75 S. Park, J. M. Joo, E. J. Cho, *Eur. J. Org. Chem.* 2015, 4093–4097.
- 76 K. S. Lee, F. Barbieri, E. Casali, E. T. Marris, G. Zanon, J. M. Schomaker, *J. Am. Chem. Soc.* 2025, **147**, 318–330.
- 77 T. Kawajiri, M. Hosoya, S. Goda, E. Sato, S. Suga, *Org. Lett.* 2025, **27**, 4737–4741.
- 78 S. Akiyama, S. Nomura, K. Kubota, H. Ito, *J. Org. Chem.* 2020, **85**, 4172–4181.



The data underlying this study are available in the published article and its ESI.

